Study of dispersion properties of hollow-core photonic crystal fiber by finite element method

S. MISHRA[*], VINOD K. SINGH
Department of Applied Physics, I.S.M.University, Dhanbad, Jharkhand, India

Dispersion properties of Hollow-core PCF or micro-structured PCFs are investigated via Finite Element Method (FEM). FEM is attractive simulation technique as it can handle complicated structure geometries very effectively. In this paper, the dispersion characteristics, mode effective refractive index, non-linear co-efficient and effective mode area of 3-ring hexagonal hollow-core PCFs have been investigated by using FEM. By suitable designing of 3-ring air holes of hollow-core photonic crystal fiber at operating wavelength from 0.65μm to 1.55μm nice modal field patterns of guided light were found. The core diameter, pitch and air hole diameter of 3-ring PCF designed in our investigation are 0.2 μm, 2.3 μm and 1.38 μm respectively. A nearly zero dispersion of the newly designed PCF is then observed at wavelength 0.98 μm.

1. Introduction

Now a day optical fibers have diverse applications in telecommunications, sensors, soliton, lasers, medical instrumentations etc. In the optical fiber, light is being guided by total internal reflection principle (TIR) [1]. There are some limitations of conventional optical fibers: for example, dispersion is normal for wavelength 1.3μm and anomalous at longer wavelengths. Optical non-linearity in conventional optical fiber is very small. To overcome these limitations of the conventional optical fiber, an alternate fiber called photonic crystal fiber (PCF) is developed [2-6]. A very important feature is that it can be made of a single material, in comparison to all other type of fibers, which are made of two or more materials. Photonic crystals are materials with periodic structure on the order of wavelength of light, i.e. nanometers. Essentially, photonic crystals contain regularly repeating internal regions of high and low dielectric constant. The governing property of these crystals is a photonic band gap: ranges of frequency for which light cannot propagate through the structure. Photonic crystal fibers (PCFs) are made from single material such as silica glass with an array of microscopic air channels running along its length. The primary difference between photonic crystal fiber and conventional fiber is that photonic crystal fibers feature an air-silica cross section, where as standard optical fibers have an all glass cross-section. Photonic crystal fibers can exhibit unique dispersion characteristics, achieve very high birefringence, provide single mode operation for very short wavelength range offer very large or low non linearity. Moreover, light can propagate through it with very low loss in certain wavelength range. The hexagonal triangular-based cladding structure is used, where refractive index of air-core and silica are 1 and 1.45 respectively. By manipulating circular air hole diameter

'd', pitch 'Λ' and air core diameter d′, it is possible to control the properties of PCF such as dispersion and leakage loss very easily.

The large variety of holes, shapes and arrangements in PCF demands the use of numerical method that can handle arbitrary cross-sectional shapes to analyze this kind of structures. Many numerical techniques have been used to analyze photonic crystal fibers, like fourier transform method, plane wave expansion method, effective index method, beam propagation method, finite time domain method. Here we have used finite element method, which is suitable for such analysis as it can handle complicated structure geometries very effectively.

2. Theory and numerical analysis

The finite element method (FEM) is generally advantageous in complex geometries of photonic crystal fiber. It is a full vector implementation for both leaky modes and cavity modes for two dimensional Cartesian cross sections in cylindrical co-ordinates. First and second order interpolant basis are provided for each triangular elements. PEC (Perfect electrical conductor) or PML (perfectly matched layer) boundary conditions selected independently for each direction. We begin with the source-free time harmonic form of the vector wave equation in an arbitrary, anisotropic lossy media[7, 8].

$$\nabla \times \left(\frac{1}{\bar{\varepsilon}_r} \cdot (\nabla \times \vec{H}) \right) - K_0^2 \bar{\mu}_r \vec{H} = 0 \tag{1}$$

Subject to vanishing field boundary conditions at the domain edges

$$\hat{n} \times \vec{E} = 0 \tag{2}$$

The complex diagonal tensors s and ε_r represent co-ordinates stretching and the dielectric material respectively. Throughout the domain s is the identity tensor, but in the boundary layer, it has the following form

$$\bar{s} = \left(\frac{s_y s_z}{s_x}\right)\hat{x}\hat{x} + \left(\frac{s_x s_z}{s_y}\right)\hat{y}\hat{y} + \left(\frac{s_x s_y}{s_z}\right)\hat{z}\hat{z}$$

$$s_{\alpha = x,y,z} = 1 - \left(\frac{\alpha-1}{L}\right)^2 \delta_{max} \qquad (3)$$

δ_{max} is the loss tangent, α is the distance from the edge and L is the thickness of the layer, known as the perfect matched layer (PML). The tensor elements in the PML are matched to those in the rest of the domain according the prescription, $\bar{\varepsilon}_r = \bar{s} \, \bar{\varepsilon}$ to produce arbitrarily small reflection at the PML interface for all frequencies and angle of incidence. The PML is terminated with a perfect electric conductor (PEC) boundary condition (eq. 3).

The finite element method does not solve the boundary value problem (eq. 1-3) directly but rather a related one based on a variational expression or functional, constructed from the operator of the differential equation (1).

This functional in two dimensions over domain A is given by

$$F(E) = \iint_A \left[(\nabla \times E) \cdot \frac{1}{\varepsilon} \cdot (\nabla \times E) - \bar{s} \cdot E \right] dA \qquad (4)$$

For propagating and leaky modes [9],a separable electric field becomes

$$E(x, y, z) = E(x, y) \exp(-j\beta z)$$

where, β is the modal propagation constant along z.

Instead of finding an expansion basis over the entire domain, which can be difficult in general, the finite element method sub-divides the domain into a collection of elements for which a simple basis can be defined. This basis vanishes outside the element, so that the final solution is just a summation over the solution of all the elements.

For hybrid node/edge FEM, the transverse components are expanded in a vector (edge element) basis.

$$\vec{E}_T(x, y) e^{-j\beta z} = \sum_{i=1}^{n} \vec{N}_i E_{Ti} = \sum_{i=1}^{n} \{U\hat{x} + V\hat{y}\} E_{Ti} \qquad (5)$$

where, E_{Ti} are the values of the field along each edge. The longitudinal component (perpendicular to the plane of the element) is represented by a scalar (node element) basis.

$$E_z(x, y) e^{-j\beta z} = \sum_{i=1}^{n} N_i E_{zi} \qquad (6)$$

where, E_{zi} are the values of the field and N_i are the basis at each node. The basis dimension n' depends on the geometry of the element and the order of the interpolation. Since the Euler Langrangian equations of the functional correspond to original wave equations the solution of latter equations can be approximated by extremization of the functional. The functionals are approximated using interpolation of polynomial basis functions and functional are discretized in a finite no. of element within the computational domain [10-23].

$$\frac{\partial F}{\partial E_i} = 0 \qquad (7)$$

Finally, we will get matrix generalized eigen-value equation of the form

$$\nabla F = (A - n_{eff}^2 B)\{E_{Ti}\} = \{0\} \qquad (8)$$

3. Results and discussions
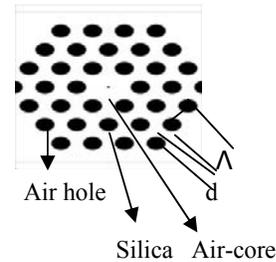
Fig. 1. (Hollow-core photonic crystal fiber); refractive index of silica and air hole are 1.45 and ,1 respectively.

(i)For Structure-1(d=1.38μm, d'=0.2μm, Λ=2.3μm),
(ii) structure-2(d=1.38μm, d'=0.3μm, Λ=2.3μm)
(iii) structure-3(d=1.38μm, d'=0.4μm, Λ=2.3μm)

We have investigated a hollow core PCF with triangular lattice of air holes shown in Fig. 1, which has three rings of air hole with same diameter d=1.38μm and pitch (distance between two center of air hole) Λ=2.3μm but different air-core (d') in the central position. The refractive index of air holes and silica are 1 and 1.45 respectively. We have varied air core d' from 0.2μm to 0.4μm keeping other parameter unchanged. By using Finite Element Method [24], we have analyzed modal field patterns and effective refractive index of the fundamental

mode at operating wavelengths from 0.65μm to 1.55μm. It is clear that the effective index n_{eff} decreases as d′ increases especially in the long wavelength region and effective refractive index is maximum as shown in Fig. 2. It is clear that modal pattern is better (effective index is maximum for this) in 1st case i.e. d′ = 0.2 μm which clearly indicates that loss of propagated light is less in 1st structure than that of other at wavelength 0.65μm and 1.55μm given in Fig. 3 and Fig. 4. It might be mentioned here that mode pattern becomes lossy at wavelength less than 0.65 μm and greater than 1.55μm.
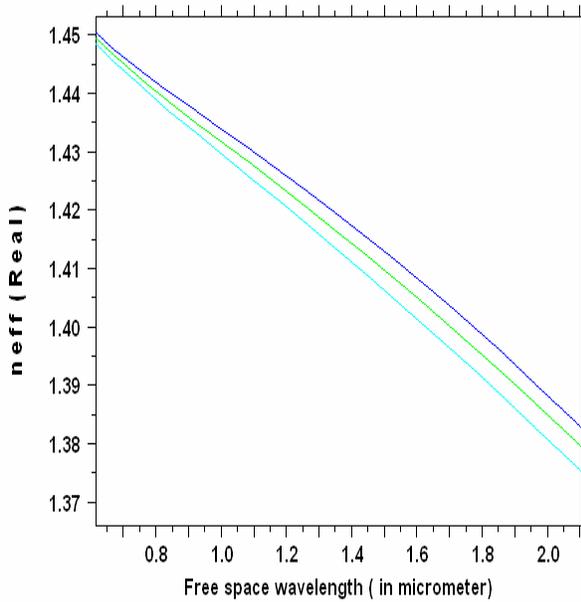
Fig. 2. Simulated effective index of the PCF with fixed pitch Λ=2.3μm and three ring holes diameter are 1.38μm for core diameter d′=0.2μm (blue), d′=0.3μm (green) and d′=0.4μm (sky blue) respectively.
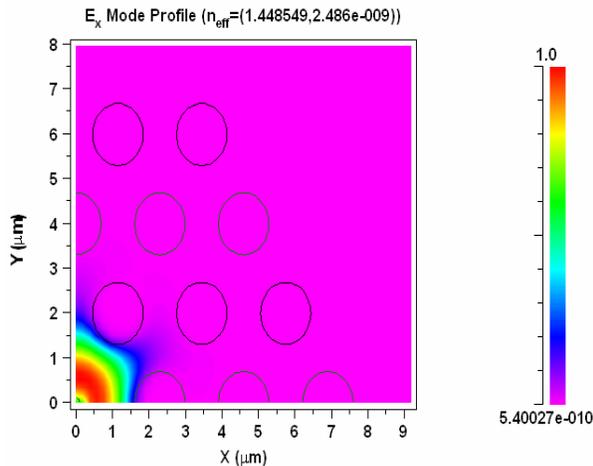
Fig. 3. Simulated transverse electric modal field pattern (one fourth part) of hollow core PCF at wavelength 0.65μm where real and imaginary refractive index are

1.448549 and 2.486-e-009 for structure-1,(all three ring air hole diameter d=1.38μm, air core diameter d′=0.2μm and pitch Λ=2.3μm).

Once the modal real effective indices are solved, the geometrical dispersion parameter D_g can be obtained as

$$D_g(\lambda) = - \left(\frac{\lambda}{c}\right)\left(\frac{d^2 R_e[n_{eff}]}{d\lambda^2}\right) \qquad (9)$$

where c is the velocity of the light in vacuum and λ is the operating wavelength, $R_e[n_{eff}]$ is the real part of effective index. The total dispersion has been calculated as the sum of the geometrical dispersion D_g (or waveguide dispersion) and the material dispersion(D_m) in the first order approximation.

$$D(\lambda) \approx D_g(\lambda) + r(\lambda)D_m(\lambda) \qquad (10)$$

where r is the confinement factor in silica, which is close to unity for most practical PCFs as the modal power is confined almost all in the silica with high refractive index. Total dispersion are calculated for three different structures having air core diameter d′=0.2 μm, 0.3 μm and 0.4 μm respectively using sellmeier equation (9,10). The zero dispersion occures for three structures under studied at wavelength 0.98μm, 1μm and 1.03μm respectively given in Fig. 5. The position of zero dispersion shifts towards greater wavelength as diameter of air-core increases. An ultra flattened dispersion of 0±30 ps/nm/km is obtained near wavelength 1.55μm.

The effective area A_{eff} and nonlinear co-efficient γ' of the hollow core PCF can also be calculated by using the equation

$$A_{eff} = \frac{\left(\iint_{-\infty}^{\infty}|E|^2 dxdy\right)^2}{\iint_{-\infty}^{\infty}|E|^4 dxdy} \qquad (11)$$

and

$$\gamma = \frac{2\pi n_2}{\lambda A_{eff}} \times 10^3 \ W^{-1}km^{-1} \qquad (12)$$

where E is the electric field, λ is the wavelength and n_2 is the non-linear refractive index. The calculated effective area A_{eff} are 1.953 μm^2 and 2.515μm^2 at wavelengths 0.65μm and 1.55μm respectively as shown in Fig. 6. The non-linear co-efficient corresponding to effective area 1.953 μm^2 is 7.177 W^{-1} km^{-1} where as for effective area 2.515μm^2 it is very high having value 14.775W^{-1}km^{-1}. Thus structure under studied is best suited for wavelength 1.55 μm.
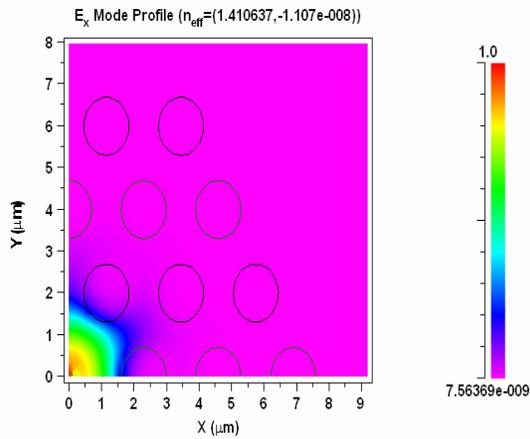
Fig. 4. Simulated transverse electric modal field pattern (one fourth part) of hollow core PCF at wavelength 1.55μm where real and imaginary effective refractive index are 1.410637 and -1.107e-008 for structure-1(all three ring air hole diameter d=1.38μm,air core diameter d'=0.2μm and pitch Λ=2.3μm).
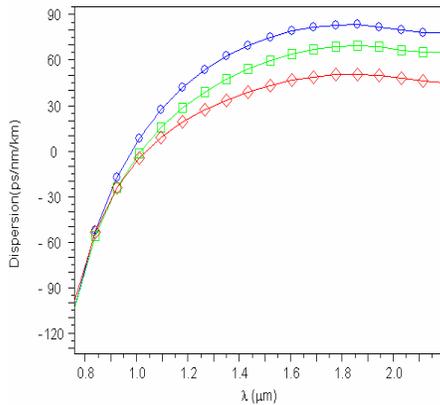
Fig. 5. Wavelength dependence of total dispersion of hollow core PCF, where Λ=2.3μm, d=1.38μm and for blue curve d'=0.2μm, for green curve d'= 0.3μm and red curve d'=0.4μm, respectively.
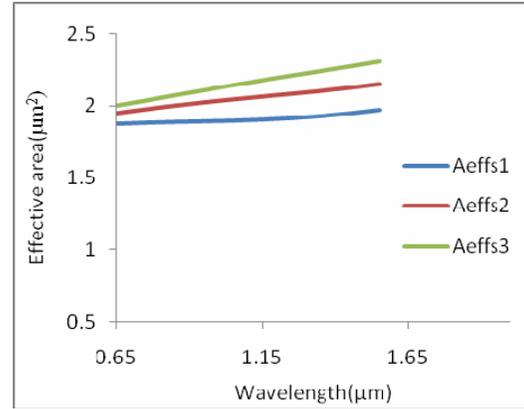
Fig. 6. Effective area of modal field pattern of hollow core PCF for three different structure where Λ=2.3μm, d'=0.2,0.3,0.4 μm and d=1.38 μm.

4. Conclusions

A 3-ring hexagonal hollow-core PCFs is proposed with fiber parameters Λ=2.3μm, d'=0.2μm and d=1.38 μm which is suitable for telecommunication. The loss of propagated light is very small for proposed structure-1 i.e. nice modal patterns for wavelengths 0.65 μm and 1.55μm are achieved. The dispersion properties of newly designed PCF are also studied and the zero dispersion is observed at wavelength 0.98 μm. Further, effective areas A_{eff} at wavelength 0.65 μm and 1.55μm are found to be 1.953 $μm^2$ and 2.515$μm^2$ respectively. The non-linear co-efficient are also calculated for two wavelengths. It is found that non-linear co-efficient $(14.775W^{-1}km^{-1})$ corresponding to the effective area 2.515$μm^2$ is large at wavelength 1.55μm. The ultra flattened dispersion of $0 \pm 30 \, ps/nm/km$ is also obtained near wavelength 1.55μm. Thus, We can conclude that an introduction of a small air-core provides us more flexibility and possibilities than index-guided PCF to obtain surprising performances and by proper designing of hollow-core photonic crystal, non lossy propagation of guided wave can be achieved.

References

[1] A. Ghatak, K. Thyagarajan, Introduction to fiber Optics, Cambridge University Press, 2002.
[2] S. G. Johnson, J. D. Joannopoulos, Photonic crystals: the road from theory to practice, Kluwer Academic Publishers, 1973.
[3] F. Zolla, G. Renversez, A. Nicolet, Foundation of Photonic Crytal Fibers, Imperial College Press publisher, 2005.
[4] P. Russell, Photonic Crystal Fibers, Review Applied Physics 17 January 2003, **299**, Science.
[5] J. C. Knight, T. A. Birks, J. P. St. Russell, D. M. Atkin, Optics letters **21**(19), 1547 (1996).
[6] S. Konar, R. Bhattacharya, Optoelectron. Adv. Mater. - Rapid Comm. **1**(9), 442 (2007).
[7] T. A.Birks, J. C. Knight, J. P. St. Russell, 1997, Optics letters **22**, 961 (1997).

[8] P. Sarrafi, A. Naqavi, K. Mehrany, S. Khorassani, B. Rashidian, Optics communications **281**(10), 2826 (2008).

[9] Y. Tsuji, M. Koshiba, IEEE JLT **18**(4), 618 (2000).

[10] F. Brechet, J. Marcou, D. Pagnoux, P. Roy, Optical fiber technology **6**(2), 181 (2000).

[11] M. Koshiba, K. Hayata, M. Suzuki, Trans. Inst. Electron. Commun. Eng. Japan, **E67,** 191 (1984).

[12] H. P. Uranus, J. W. Hoekstr, Opt. Express **12**(12), 2795 (2004).

[13] S. Mishra, V. K. Singh, V. Priye, Proceeding of National Seminar held at I.S.M. University, Dhanbad on 15-17 Feb. 2007, page 83.

[14] S. Mishra, V. K. Singh, V. Priye, Proceeding of National Seminar held at I.S.M. University, Dhanbad on 13-15 Oct. 2008, page 95.

[15] S. Mishra, V. K. Singh, Proceeding International conference "Photonics 2008" held at IIT Delhi on 15-18, Dec. 2008 Page 242, 2008.

[16] J. Jin, The, Finite Element Method in Electromagnetics, 2nd Ed.,John Wiley & Sons, New York, 2002.

[17] S. Saitoh, M. Koshiba, IEEE JQE **38**(7), 927(2002).

[18] D. Schulz, C. Glingener, M. Bludszuweit, E. Voges, IEEE JLT **16**(7), 1336 (1998).

[19] Qin-Ling Zhou, Xing-Qiang Lu, Dan-Ping Chen, Cong-Shan Zhu, Jian-Rong Qiu, Journal of Non-Crystalline solids, **354** (12-13), 1201 (2008).

[20] Y. Tsuji, M. Koshiba, T. Shiraishi, IEEE JLT, **15**(9), 1728 (1997).

[21] M. Koshiba, Y. Tsuji, IEEE JLT **18**(5), 737 (2000).

[22] A. F. Peterson, IEEE Trans. on Antennas and propagation **43**(3), 357 (1994).

[23] J. C. Nedelec, Numerische Mathematik **35**, 315 (1980).

[24] FEMSIM 1.3.2003. Rsoft Design Group, Ossining, NY 10562.

_____
*Corresponding author: suvendumohan_2006@yahoo.co.in